Synthesis and Characterization of Adducts of Alachlor and 2-Chloro-*N*-(2,6-diethylphenyl)acetamide with 2′-Deoxyguanosine, Thymidine, and Their 3′-Monophosphates[1]

Stephen Nesnow,*,† Satish C. Agarwal,‡ William T. Padgett,§ Guy R. Lambert,§ Phillip Boone,§ and Ann M. Richard†

Carcinogenesis and Metabolism Branch (MD-68), Health Effects Research Laboratory, U.S. Environmental Protection Agency, Research Triangle Park, North Carolina 27711, Environmental Health Research and Testing, Research Triangle Park, North Carolina 27709, and Integrated Laboratory Systems, Inc., Research Triangle Park, North Carolina 27709

Received September 1, 1994⊗

Adducts of the preemergence herbicide 2-chloro-*N*-(methoxymethyl)-*N*-(2,6-diethylphenyl)-acetamide (alachlor) and 2-chloro-*N*-(2,6-diethylphenyl)acetamide (CDEPA) with 2′-deoxyguanosine, thymidine, 2′-deoxyguanosine 3′-monophosphate, and thymidine 3′-monophosphate have been synthesized and characterized. Under mildly basic conditions alachlor and CDEPA form N-1 adducts with 2′-deoxyguanosine and N-3 adducts with thymidine as a result of chlorine displacement. In addition, alachlor formed an N-7 adduct with 2′-deoxyguanosine, 7-[[(*N*-(methoxymethyl)-*N*-(2,6-diethylphenyl)carbamoyl]methyl]guanine. N-1 adducts of alachlor and CDEPA with 2′-deoxyguanosine 3′-monophosphate and N-3 adducts with thymidine 3′-monophosphate are also described. In addition to spectroscopic data, structural proof included the dephosphorylation of each nucleotide adduct to its corresponding nucleoside adduct by nuclease P1. Alachlor and alachlor adducts but not CDEPA and CDEPA adducts exhibited rotational isomerism as evidenced by proton and ^{13}C NMR studies. These rotamers were attributed to hindered rotation about the shortened N-carbonyl bond. Computational methods employing molecular mechanics and quantum mechanics were used to characterize the structures and energies of these rotamers to account for the patterns of duplicate NMR resonances observed.

Introduction

Alachlor (**1a**) [2-chloro-*N*-(methoxymethyl)-*N*-(2,6-diethylphenyl)acetamide] is a widely used preemergence herbicide employed for the control of weeds in corn and soybeans. Over 70 million pounds are used annually (*1*). Exposure to alachlor, particularly among farmers, can come from several media including air and water. Alachlor and its metabolites have been detected in the urine of pesticide applicators (*2*).

Alachlor induces DNA single strand breaks in isolated rat hepatocytes (*3*) and induces nasal and stomach tumors in rats and lung tumors in mice after lifetime oral administration (*4, 5*). The metabolism of alachlor in vivo and in vitro is complex, involving O-dealkylation, benzylic oxidation, and GSH conjugation (*6*). Two of the major metabolites are 2-chloro-*N*-(2,6-diethylphenyl)acetamide (**1b**, CDEPA)[2] and diethylaniline. Brown *et al.* (*7*) have reported that alachlor, CDEPA, and diethylaniline bind to mouse liver DNA and hemoglobin protein. Using alachlor [^{14}C]-labeled in the phenyl and methoxy carbons, their data suggested that binding could occur directly from alachlor or CDEPA, by further metabolic activation of diethylaniline, or by formaldehyde liberated in the conversion of alachlor to CDEPA. They also reported preliminary findings on the characterization of a CDEPA–2′-deoxyguanosine adduct.

The ability of alachlor and CDEPA to bind to DNA, alachlor's genotoxic and carcinogenic activities, and the potential for widespread exposure to alachlor has prompted us to synthesize specific alachlor and CDEPA adducts with nucleosides and nucleotides. On the basis of the work of Brown *et al.* (*7*) we selected 2′-deoxyguanosine and thymidine and their 3′-monophosphates as target nucleosides and nucleotides. Our results provide the details of the syntheses and full characterization of a number of adducts of alachlor and CDEPA with 2′-deoxyguanosine and thymidine and their 3′-monophosphates.

Materials and Methods

Chemicals. Alachlor was purchased from Chem Service (Westchester, PA), organic intermediates and solvents were from Aldrich Chemical Co. (Milwaukee, WI), and 2′-deoxyguanosine, thymidine, their 3′-monophosphates, and nuclease P1 were from Sigma Chemical Co. (St. Louis, MO). **Caution:** *Chloroacetyl chloride is hazardous, reacting violently with water or protonic compounds, and should be handled carefully.*

* Address correspondence to this author at the Carcinogenesis and Metabolism Branch (MD-68), Health Effects Research Laboratory, U.S. Environmental Protection Agency, Research Triangle Park, NC 27711.
† U.S. Environmental Protection Agency.
‡ Environmental Health Research and Testing.
§ Integrated Laboratory Systems, Inc.
⊗ Abstract published in *Advance ACS Abstracts*, February 1, 1995.
[1] This article has been reviewed by the Health Effects Research Laboratory, U.S. EPA, and approved for publication. Mention of trade names or commercial products should not be construed as endorsement or recommendation for use.

[2] Abbreviations: CDEPA, 2-chloro-*N*-(2,6-diethylphenyl)acetamide; COSY, correlated spectroscopy ($^1H-^1H$); DEPT, distortionless enhanced polarization transfer (^{13}C); GMP(3′), 2′-deoxyguanosine 3′-monophosphate; TMP(3′), thymidine 3′-monophosphate, XHCORR, heteronuclear ($^1H-^{13}C$) correlation spectroscopy.

0893-228x/95/2708-0209$09.00/0

Apparatus. Melting points were taken on a Thomas-Hoover capillary apparatus and are uncorrected. UV spectra were determined on a Beckman Model DU-70. NMR spectra were recorded on a Bruker ACF-300 instrument at 300.13 MHz for ^1H and 75.49 MHz for ^{13}C. Chemical shifts are reported as ppm referenced to TMS. 2D-COSY, 2D-XHCORR, long-range 2D-XHCORR, and DEPT spectra were recorded according to established manufacturer's protocols. Low resolution mass spectra were obtained on an Extrel ELQ-400-3X triple quadrapole mass spectrometer. Sample introduction by LC/MS was achieved using an Eldex Model 9600 HPLC equipped with an Applied Biosystems Spheri-5 RP-18 cartridge column (2.1 × 250 mm) via Extrel's Thermabeam interface. Ionization was by chemical ionization using methane. Perfluorotributylamine was used as the mass calibration standard. Exact mass determinations were recorded on a VG70-250SEQ hybrid mass spectrometer at 10 000 resolution by liquid SIMS in a glycerol matrix using a cesium ion gun. The spectra were acquired over a range encompassing the mass of the analyte and two poly(ethylene glycol) reference peaks bracketing the mass of the analyte. Microanalyses were performed by Galbraith Laboratories, Inc. (Knoxville, TN). Analytical and preparative TLC was carried out on precoated fluorescent silica gel plates. Bands were visualized with short- and long-wavelength UV lamps. Silica gel (70–230 mesh ASTM) or Whatman LRP-2 bulk microparticle media was used for column chromatography for the separation of adducts. HPLC was conducted on a Shimazdu Model 10A HPLC connected to a Hewlett-Packard Model 1050 diode array detector. Effluents were monitored over the range of 220–550 nm.

2-Chloro-*N*-(2,6-diethylphenyl)acetamide (1b). To a stirred solution of freshly distilled 2,6-diethylaniline (30 g, 0.2 mol) in anhydrous ethyl acetate (250 mL) was added dropwise chloroacetylchloride (44 g, 0.4 mol) from an addition funnel fitted to a three-necked flask with a condenser and an N_2 inlet tube. The solution was heated under reflux for 2 h under N_2 atmosphere. A white precipitate appeared during the reaction. Ethyl acetate was distilled off under reduced pressure, and ice-cold water was added to the oily residue and extracted with CH_2Cl_2 (300 mL). The organic layer was washed with water (3 × 250 mL), dried over $MgSO_4$, filtered, and concentrated by evaporation. Sufficient hexane was added to the concentrate to allow crystallization at 4 °C that gave colorless needles (44.6 g, 99.1% yield): mp 131–133 °C ; MS *m/z* (relative intensity): 225 $[M]^+$ (8.6), 176 $[M - CH_2Cl]^+$ (100), 161 $[M - HCOCl]^+$ (10.0), 148 $[M - COCH_2Cl]^+$ (25.7), 134 $[M\text{-}NCOCH_2Cl]^+$ (16.3); ^1H-NMR ($CDCl_3$) δ 1.22 (t, 6H, $2CH_3CH_2$), 2.6 (q, 4H, $2\text{-}CH_3CH_2$), 4.25 (s, 2H, $COCH_2Cl$), 7.15–7.28 (m, 3H, phenyl), 7.85 (s, 1H, NH exchangeable with D_2O). Anal. Calcd for $C_{12}H_{16}NOCl$: C, 63.84; H, 7.16; N, 6.21. Found: C, 63.89; H, 7.27; N, 6.12.

1-[[*N*-(Methoxymethyl)-*N*-(2,6-diethylphenyl)carbamoyl]methyl]-2′-deoxyguanosine (2a). Alachlor (**1a**) (1.0 g, 3.71 mmol) and 2′-deoxyguanosine (1.0 g, 3.74 mmol) were combined in 2-methoxyethanol (150 mL). After the addition of 1.5 mL of saturated sodium bicarbonate the reaction mixture was incubated at 50 °C for 15 days. The reaction mixture was filtered, and the filtrate was absorbed onto silica gel and applied to a column of silica gel in $CHCl_3$. Initial elution with $CHCl_3$ removed unreacted **1a**. This was followed by 8:1 $CHCl_3/CH_3OH$ which eluted the adduct of R_f 0.58 on silica gel plates in 4:1 $CHCl_3/CH_3OH$. Rotary evaporation afforded **2a** as a colorless amorphous solid (220 mg, 12%) that did not melt below 300 °C. UV (methanol) λ_{max} 256 nm (ε 12 700), 276 (sh). Anal. Calcd for $C_{24}H_{32}N_6O_6 \cdot {}^1/_4H_2O$: C, 57.06; H, 6.50; N, 16.64. Found: C, 57.16; H, 6.67; N, 16.60. High resolution MS, $(M + H)^+$ $C_{24}H_{32}N_6O_6$: calcd 501.2462, observed 501.2474.

7-[[*N*-(Methoxymethyl)-*N*-(2,6-diethylphenyl)carbamoyl]methyl]guanine (3). The reaction mixture from the formation of **2a** was evaporated and taken up in CH_3OH. The insoluble material was filtered and washed with CH_3OH. It was then washed with H_2O and again with CH_3OH followed by drying under vacuum desiccation over P_2O_5 to give a colorless amorphous solid (87 mg, 6.1% yield) that did not melt below 300 °C. UV (2 N HCl) λ_{max} 252 nm (ε 9353); MS *m/z* (relative intensity): 385 $[M + H]^+$ (16.8), 204 $[C_{10}H_{13}N(CO)CO + H]^+$ (62.7), 162 $[C_{10}H_{13}NCH_2 + H]^+$ (100), 114 (22.2). Anal. Calcd for $C_{19}H_{23}N_6O_3$: C, 59.51; H, 6.06; N, 21.92. Found: C, 59.16; H, 6.31; N, 21.70.

1-[[*N*-(2,6-Diethylphenyl)carbamoyl]methyl]-2′-deoxyguanosine (2b). CDEPA (**1b**) (1.0 g, 4.44 mol) and 2′-deoxyguanosine (1.0 g, 3.74 mmol) were combined in 2-methoxyethanol (150 mL) and were heated initially at reflux for 30 min. The suspension was cooled to room temperature, and saturated sodium bicarbonate (1.5 mL) was added, resulting in some precipitate formation. The reaction mixture was kept at 45–50 °C for 14 days. The reaction mixture was filtered, and the filtrate was absorbed onto silica gel and applied to a column of silica gel in $CHCl_3$. Initial elution with $CHCl_3$ removed unreacted **1b.** This was followed by 10:1 $CHCl_3/CH_3OH$ which eluted **2b** with an R_f 0.78 on silica gel plates (4:1 $CHCl_3/CH_3OH$). Evaporation afforded **2b** as a colorless amorphous solid (216 mg; 12% yield) that did not melt below 300 °C. UV (methanol) λ_{max} 256 nm (ε 16 600); 276 (sh). Anal. Calcd for $C_{22}H_{28}N_6O_5 \cdot {}^1/_4H_2O$: C, 57.31; H, 6.24; N, 18.23. Found C, 57.39; H, 6.39; N, 18.06. High resolution MS, $(M + H)^+$ $C_{22}N_{28}N_6O_5$: calcd 457.2199, observed 457.2220.

3-[[*N*-(Methoxymethyl)-*N*-(2,6-diethylphenyl)carbamoyl]methyl]thymidine (4a). **1a** (1.0 g, 3.71 mmol) and thymidine (1.0 g, 4.14 mmol) were combined in 2-methoxyethanol (150 mL) and were heated initially at reflux for 30 min. The reaction mixture was cooled to room temperature, and saturated sodium bicarbonate (1.5 mL) was added, resulting in some precipitate formation. The reaction mixture was kept at 45–50 °C for 14 days. The reaction mixture was filtered, and the filtrate was absorbed onto silica gel and applied to a column of silica gel in $CHCl_3$. Initial elution with $CHCl_3$ removed unreacted **1a**. This was followed by 10:1 $CHCl_3/CH_3OH$ which eluted **4a** with an R_f 0.72 on silica gel plates (4:1 $CHCl_3/CH_3OH$). Evaporation afforded **4a** as a colorless amorphous solid (330 mg, 5.3% yield) that did not melt below 300 °C. UV (methanol) λ_{max} 267 nm (ε 7030). Anal. Calcd for $C_{24}H_{33}N_3O_7$: C, 60.61; H, 7.01; N, 8.84. Found: C, 60.75; H, 7.30; N, 8.65.

3-[[*N*-(2,6-Diethylphenyl)carbamoyl]methyl]thymidine (4b). **1b** (1.0 g, 4.44 mmol) and thymidine (1.0 g, 4.14 mmol) were combined in 2-methoxyethanol (150 mL) and were heated initially at reflux for 30 min. The suspension was cooled to room temperature, and saturated sodium bicarbonate (1.5 mL) was added, resulting in some precipitate formation. The reaction mixture was kept at 45–50 °C for 14 days. The reaction mixture was filtered, and the filtrate was absorbed onto silica gel and applied to a column of silica gel in $CHCl_3$. Initial elution with $CHCl_3$ removed unreacted **1b**. This was followed by 10:1 $CHCl_3/CH_3OH$ which eluted **4b** with an R_f 0.84 on silica gel plates in 4:1 $CHCl_3/CH_3OH$. Evaporation afforded **4b** as a colorless amorphous solid (458 mg, 26% yield): mp 225–226 °C; UV (methanol) λ_{max} 267 nm (ε 8990). Anal. Calcd for $C_{22}H_{29}N_3O_6$: C, 61.23; H, 6.79; N, 9.74. Found: C, 61.42; H, 6.57; N, 9.67. High resolution MS, $(M + H)^+$ $C_{22}H_{29}N_3O_6$: calcd 432.2135, observed 432.2133.

1-[[*N*-(Methoxymethyl)-*N*-(2,6-diethylphenyl)carbamoyl]methyl]-2′-deoxyguanosine 3′-Monophosphate (2c). **1a** (1.6 g, 5.95 mmol) was dissolved in 150 mL of 2-methoxyethanol. 2′-Deoxyguanosine 3′-monophosphate (as the ammonium salt) (100 mg, 0.262 mmol) and sodium bicarbonate (50 mg, 0.592 mmol) were dissolved in 150 mL of water. The two solutions were combined, at which point a precipitate appeared. The reaction mixture was heated to 50 °C, and the solution became clear. After 48 h the reaction was terminated by cooling, the reaction mixture was freeze-dried, and the residue was triturated several times with CH_2Cl_2 to remove unreacted **1a**. The residue was dissolved in water and chromatographed by medium pressure on Whatman LRP-2. Fractions were eluted with water and were analyzed by HPLC using a 4.6 × 250 mm Synchrom Synchropak RPP-18 column (300 Å pore size) with a guard column in place. Solvent A, 0.25 M KH_2PO_4 (pH 5.52); solvent B, CH_3CN; flow rate, 1.0 mL/min; linear gradient elution

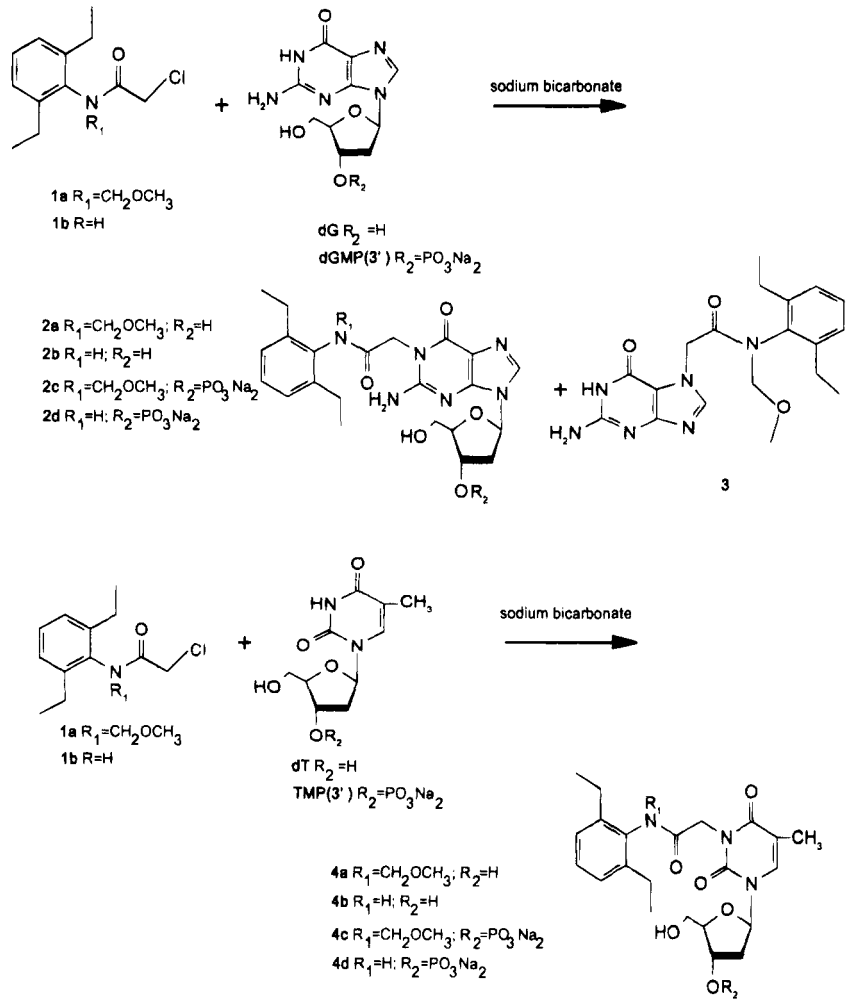

Figure 1. Reaction scheme and structures of alachlor and CDEPA adducts.

scheme (segment no.; time, min; initial concentration, % B in A; final concentration, %B in A): 1, 1, 0, 0; 2, 20, 0, 60; 3, 6, 60, 60. Fractions containing pure **2c** eluted at 19.2 min and were combined and evaporated to give the product as a colorless amorphous solid (14.7 mg, 9.13% yield). UV (water) λ_{max} 254 nm (ϵ 7605). Several passes through a Bio-Rad AG 50W-X8 (Na form) converted **2c** into its sodium form.

1-[[*N*-(2,6-Diethylphenyl)carbamoyl]methyl]-2′-deoxyguanosine 3′-Monophosphate (2d). 1b (100 mg, 0.444 mmol) was dissolved in 75 mL of 2-methoxyethanol. 2′-Deoxyguanosine 3′-monophosphate (100 mg, 0.255 mmol) and sodium bicarbonate (50 mg, 0.592 mmol) were dissolved in 50 mL of water. The two solutions were combined, at which point a precipitate appeared. The reaction mixture was heated to 75 °C, and the solution became clear. After 24 h the reaction was terminated by cooling, the reaction mixture was freeze-dried, and the residue was triturated several times with CH_2Cl_2 to remove unreacted **1b**. The residue was dissolved in water and chromatographed by medium pressure on Whatman LRP-2. Fractions were eluted with water and were analyzed by HPLC using a 4.6 × 250 mm Synchrom Synchropak RPP-18 column (300 Å pore size) with a guard column in place. Solvent A, 0.25 M KH_2PO_4 (pH 5.52); solvent B, CH_3CN; flow rate, 1.0 mL/min; linear gradient elution scheme (segment no.; time, min; initial concentration, % B in A; final concentration, %B in A): 1, 1, 0, 0; 2, 20, 0, 60; 3, 6, 60, 60. Fractions containing pure **2d** eluted at 16.5 min and were combined and evaporated to give the product as a colorless amorphous solid (21.4 mg, 14.7% yield). UV (water) λ_{max} 254 nm (ϵ 16 700).

3-[[*N*-(Methoxymethyl)-*N*-(2,6-diethylphenyl)carbamoyl]-methyl]thymidine 3′-Monophosphate (4c). 1a (100 mg, 0.371 mmol) was dissolved in 3 mL of 2-methoxyethanol. Thymidine 3′-monophosphate (100 mg, 0.272 mmol) and sodium bicarbonate (50 mg, 0.592 mmol) were dissolved in 3 mL of water. The two solutions were combined, at which point a precipitate appeared. The reaction mixture was heated to 75 °C, and the solution became clear. After 24 h the reaction was terminated by cooling, the mixture was freeze-dried, and the residue was triturated several times with CH_2Cl_2 to remove unreacted **1a**. The residue was dissolved in water and chromatographed by medium pressure on Whatman LRP-2. Fractions were eluted with water and then methanol. Fractions were analyzed by HPLC using a 4.6 × 250 mm Synchrom Synchropak RPP-18 column (300 Å pore size) with a guard column in place. Solvent A, 0.25 M KH_2PO_4 (pH 5.52); solvent B, CH_3CN; flow rate, 1.0 mL/min; linear gradient elution scheme (segment no.; time, min; initial concentration, % B in A; final concentration, %B in A): 1, 1, 0, 0; 2, 20, 0, 60; 3, 6, 60, 60. Fractions containing pure **4c** eluted at 20.4 min and were combined and evaporated to give the product as a colorless amorphous solid (17.3 mg, 10.8% yield). UV (water) λ_{max} 267 nm (ϵ 6560). High resolution MS, $(M + H)^+$ $C_{24}H_{34}N_3O_{10}PNa$: calcd 578.1879, observed 578.1949.

3-[[*N*-(2,6-Diethylphenyl)carbamoyl]methyl]thymidine 3′-Monophosphate (4d). 1b (100 mg, 0.444 mmol) was dissolved in 15 mL of 2-methoxyethanol. Thymidine 3′-monophosphate (100 mg, 0.272 mmol) and sodium bicarbonate (46 mg, 0.547 mmol) were dissolved in 15 mL of water. The two solutions were combined, at which point a precipitate appeared. The reaction mixture was heated to 82 °C, and the solution became clear. After 24 h the reaction was terminated by cooling, the mixture was freeze-dried, and the residue was triturated several times with CH_2Cl_2 to remove unreacted **1b**. The residue was dissolved in water and chromatographed by medium pressure on Whatman LRP-2. Fractions were eluted with water and then increasing concentrations of CH_3CN/water.

Table 1. Mass Spectral Fragmentation Patterns Common to Alachlor and CDEPA Adducts[a]

m/z (rel intensity)				
2a	**2b**	**4a**	**4b**	fragment[b]
501 (5.0)	457 (4.8)	476 (0.6)	432 (30.8)	$(M + H)^+$
413 (10.8)	369 (2.5)	388 (2.2)	344 (8.0)	$(M - A + H)^+$
385 (52.9)	341 (14.1)	360 (0.2)	316 (63.2)	$(M - B + H + H)^+$
367 (9.3)	323 (1.3)	342 (0.2)	298 (6.5)	$(M - D - H + H)^+$
308 (27.1)	308 (4.7)	283 (41.2)	283 (5.2)	$(M - C - H + H)^+$
194 (1.9)	150 (100)	194 (0.3)	150 (7.6)	$(C + H + H)^+$
192 (100)	192 (41.4)	167 (100)	167 (100)	$(M - B - C + H)^+$
134 (5.4)	134 (12.4)	134 (1.0)	134 (0.4)	$(D + H)^+$
117 (24.9)	117 (3.2)	117 (5.4)	117 (8.1)	$(B - H + H)^+$

[a] Mass spectral analyses were performed by chemical ionization using methane. Relationships between fragments were confirmed by MS–MS techniques using electron impact. [b] Fragments A–D are depicted in Figure 2.

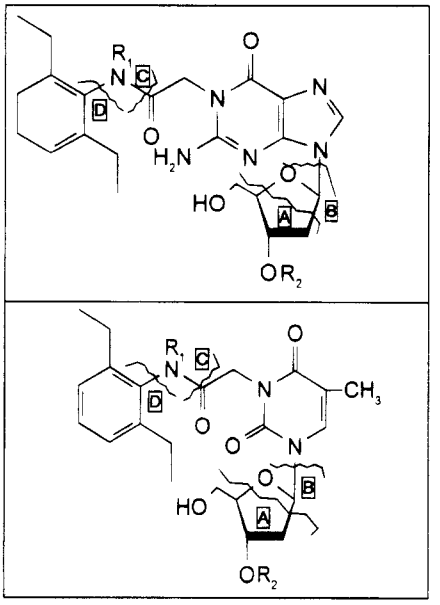

Figure 2. Common mass spectral fragment patterns of 2′-deoxyguanosine- (upper panel) and thymidine adducts (lower panel) of alachlor and CDEPA.

Fractions were analyzed by HPLC using a 4.6 × 250 mm Synchrom Synchropak RPP-18 column (300 Å pore size) with a guard column in place. Solvent A, 0.25 M KH_2PO_4 (pH 5.52); solvent B, CH_3CN; flow rate, 1.0 mL/min; linear gradient elution scheme (segment no.; time, min; initial concentration, % B in A; final concentration, %B in A): 1, 1, 0, 0; 2, 20, 0, 60; 3, 6, 60, 60. Fractions containing pure **4d** eluted at 16.4 min and were combined and evaporated to give the product as a colorless amorphous solid (53.5 mg, 36.2% yield). UV (water) λ_{max} 267 nm (ϵ 5650). High resolution MS, $(M + H)^+$ $C_{22}H_{30}N_3O_9PNa$: calcd 534.1617, observed 534.1614.

Dephosphorylation of Nucleotide Adducts. Each nucleotide adduct was subjected to nuclease P1 dephosphorylation (*8*). The nucleotide adduct (0.25–0.50 mg) was dissolved in 0.5 mL of 0.25 M sodium acetate buffer (pH 5.0), containing 0.18 mM zinc chloride. Nuclease P1 (125 units) was dissolved in 0.5 mL of water and added to the nucleotide adduct solution, and the mixture was incubated at 37 °C for 2 h. The incubation mixture was filtered through a Microcon microconcentrator with a molecular weight cutoff of 3000 (Amicon, Beverly, MA). The filtrate was analyzed by HPLC using a 4.6 × 250 mm Synchrom Synchropak RPP-18 column (300 Å pore size) with a guard column in place. Solvent A, 0.25 M KH_2PO_4 (pH 5.52); solvent B, CH_3CN; flow rate, 1.0 mL/min; linear gradient elution scheme (segment no.; time, min; initial concentration, % B in A; final concentration, %B in A): 1, 1, 0, 0; 2, 20, 0, 60; 3, 6, 60, 60.

Molecular Modeling Studies. Structures corresponding to various rotameric forms of the studied molecules were entered graphically within the SPARTAN molecular modeling program (Version 3.04, Wavefunction, Inc., Irvine, CA) on a Silicon Graphics INDIGO 4000XZ workstation, and energy minimized using the Sybyl molecular mechanics force field (Tripos Associates, St. Louis, MO). Further energy minimization of distinct rotamers was performed using a random conformational search for **1a** and **1b**, a restricted conformational search (sampling various relative starting orientations of the 2′-deoxyguanosine plane relative to the phenyl plane) for **2a** and **2b**, and semiempirical Hamiltonians, AM1 (*9*) and PM3 (*10*), as implemented within SPARTAN. Single point energy calculations were performed at the ab initio HF/6–31G* level using SPARTAN or GAUSSIAN92 (*11*), or at the density functional theory DND (double numeric plus *d* functions) level using DMol (*12*). All computations involving the use of GAUSSIAN92 or DMol were performed on a Cray Y-MP located at the EPA–National Environmental Supercomputer Center in Bay City, MI.

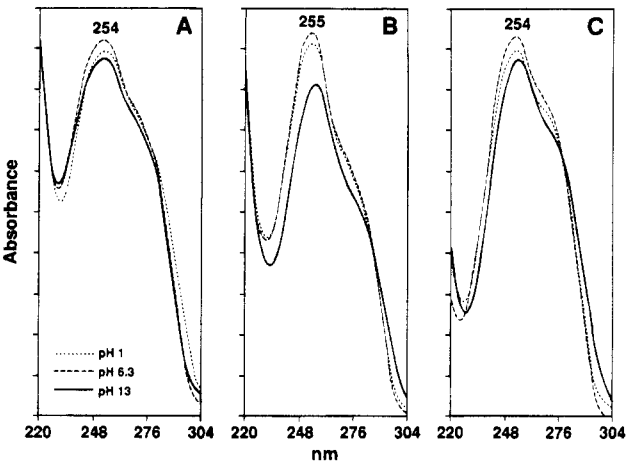

Figure 3. UV analyses of alachlor– and CDEPA–2′-deoxyguanosine adducts at different pHs. Panel A: **2a**. Panel B: **2b**. Panel C: 1-methyl-2′-deoxyguanosine. Both adducts were stable under the pH conditions used to obtain the spectra.

Results and Discussion

The synthetic route to covalent adducts between alachlor or CDEPA and 2′-deoxyguanosine, dGMP(3′), thymidine, and TMP(3′) was based on the observations of Brown *et al.* (*7*) and Grabow *et al.* (*13*) on the displacement of the chlorine atom of alachlor and CDEPA by nucleophiles under mildly basic conditions. Reaction of alachlor and CDEPA with 2′-deoxyguanosine in 2-methoxyethanol in the presence of sodium bicarbonate gave N-1-substituted products (**2a, 2b**) (Figure 1). Mass spectral analyses revealed 4 common fragmentation patterns resulting from fission within the deoxyribose ring (A), at the glycosidic bond (B), and on either side of amide nitrogen (C and D) (Table 1, Figure 2). Assignment of N-1 substitution for both products was based on analyses of the UV spectra at varying pHs. Both **2a** and **2b** exhibited absorption maxima and minima consistent with an N-1-substituted guanosine and identical to those of the reference standard, 1-methyl-2′-deoxyguanosine (Figure 3). Proton and ^{13}C NMR spectra of **2a** and **2b** revealed all the expected resonances, and atom assignments were made with 2D-COSY, 2D-XHCORR, DEPT, and long range 2D-XHCORR evaluations (Tables 2 and 3). The aromatic multiplet in these adducts (as well as in alachlor and CDEPA) presented as an AB_2 pattern with $J_{3(5),4} = 5.13$ Hz (*14*).

The alachlor-N1-2′-deoxyguanosine product, **2a,** presented many duplicate proton and ^{13}C resonances, particularly noticeable for the ethyl, $NCOCH_2N$, OCH_2N,

Table 2. Proton Magnetic Resonance Spectral Data of Alachlor and CDEPA Adducts

assignment	chemical shift, ppm				
	2b[a]	**2a**[a,b]	**3**[c,d]	**4b**[a]	**4a**[e,f]
CH_3CH_2-	1.11 (t, J = 7.5 Hz)	1.04 (t, J = 7.5 Hz) 1.21 (t, J = 7.5 Hz)	1.08 (t, J = 7.5 Hz) 1.25 (t, J = 7.5 Hz)	1.11 (t, J = 7.5 Hz)	1.1−1.4 (m)
CH_3CH_2-	2.55 (q, J = 7.5 Hz)	2.41−2.71 (m)	2.48−2.58 (m) 2.61−2.80 (m)	2.53 (q, J = 7.5 Hz)	2.70 (q,J = 7.5 Hz) 2.50−2.55 (m)
phenyl (H-3, H-4, H-5)	7.06−7.16 (m, $J_{3(5),4}$ = 5.13 Hz)	7.08−7.38 (m)	7.10−7.42 (m)	7.07−7.21 (m, $J_{3(5),4}$ = 5.13 Hz)	7.23−7.38 (m)
$COCH_2N$	4.85 (s)	4.22 (s) 5.17 (s)	4.54 (s) 5.46 (s)	4.65 (s)	4.17 (s)
CH_3O-		3.27 (s) 3.31 (s)	3.33 (s) 3.36 (s)		3.40 (s) 3.35 (s)
OCH_2N		4.78 (s) 4.89 (s) 4.89 (s)	4.84 (s) 4.92 (s)		5.04 (s)
H-1′dR	6.14 (m)	6.12 (t, J = 6.78 Hz)		6.23 (t, J = 6.62 Hz)	6.16 (t, J = 6.62 Hz)
H-2′,2″dR	2.20 (m); 2.50 (m)	2.20−2.26 (m)		2.15 (m)	2.25−2.35 (m)
H-3′dR	4.35 (m)	4.32−4.42 (m)		4.28 (m)	4.44−4.49 (m)
H-4′dR	3.80 (m)	3.80−3.85 (m)		3.82 (m)	3.89−3.92 (m)
H-5′dR	3.54 (m)	3.47−3.59 (m)		3.62 (m)	3.73−3.86 (m)
NH	9.43 (s)			9.36 (s)	
OH-3′dR	5.29 (d, J = 3.83 Hz)	5.12 (m)		5.19 (d, J = 4.27 Hz)	
OH-5′dR	4.90 (t)			4.97 (t, J = 5.1 Hz)	
H-8dGuo	7.95 (s)	7.88 (s) 7.89 (s)	7.75 (s) 7.84 (s)		
NH_2dGuo	7.05 (s)	6.5 (s)			
CH_3dT				1.88 (m)	1.88 (d, J =1.2 Hz) 1.91 (d, J = 1.2 Hz)
H−6dT				7.82 (m)	7.45 (m)

[a] Samples were dissolved in deuterated DMSO. [b] The ratio of rotamers is 2:1. [c] Samples were dissolved in deuterated DMSO with a trace of deuterated acetic acid. [d] The ratio of rotamers is 3:1. [e] Samples were dissolved in deuterated methylene chloride. [f] The ratio of rotamers is 10:1.

Table 3. ^{13}C Magnetic Resonance Spectral Data of Alachlor and CDEPA Adducts

assignment	chemical shift, ppm			
	2b[a]	**2a**[a]	**4b**[a]	**4a**[b]
CH_3CH_2-	15.1	14.2; 14.7	14.6	14.6
CH_3CH_2-	24.6	22.9; 23.6	24.2	23.9
phenyl (C-3, C-5)	126.4	126.3; 127.0	125.9	127.3
phenyl (C-4)	127.8	128.0; 129.0	126.9	129.6
phenyl (C-1)	135.0	137.1	135.0	137.5
phenyl (C-2, C-6)	142.1	139.4	141.7	142.7
$NHCOCH_2N$	44.3	43.0; 44.0	42.9	43.6
$NHCOCH_2N$	166.4	167.5; 168.1	162.5	163.4
CH_3O-		55.9; 57.1		57.8
OCH_2N		79.7; 81.9		80.7
C-1′dR	82.9	82.5	84.9	86.9
C-2′dR	40.3	40.1	39.5	40.5
C-3′dR	71.1	70.7	70.3	71.4
C-4′dR	87.8	87.6	87.5	87.4
C-5′dR	61.9	61.7	61.3	62.5
C-2dGuo	154.7	154.2; 154.7		
C-4dGuo	149.7	149.1; 149.3		
C-5dGuo	116.1	115.8; 116.1		
C-6dGuo	156.9	156.5; 156.6		
C-8dGuo	133.5	141.4; 142.5		
CH_3dT			12.8	13.4
C-2dT			150.4	151.2
C-4dT			165.9	169.1
C-5dT			108.4	110.2
C-6dT			133.5	135.5

[a] Samples were dissolved in deuterated DMSO. [b] Samples were dissolved in deuterated methylene chloride.

Table 4. Computed Relative Energies of Endo and Exo Rotamers of Alachlor and CDEPA

optimized geometry[a]	energy calculation method[b]	**1a**, ΔE_{min}[c]	**1b**, ΔE_{min}[c]	Δ-(ΔE_{min})[d]
AM1	HF-631G*	−3.47	4.59	1.12
	DMol-DND	−2.99	3.47	0.48
PM3	HF-631G*	−2.82	9.30	6.48
	DMol-DND	−1.56	4.48	2.92
HF-631G*	HF-631G*	−0.78	4.25	3.47
DMol-DND	DMol-DND	−3.36	5.53	1.93

[a] Methods used to obtain fully optimized, minimum energy geometries of rotamers with amide correction for AM1 and PM3. [b] Methods used to compute single point energies of optimized geometries. All energies in kcal/mol. [c] Difference in minimum energies, $\Delta E_{min} = E_{exo} - E_{endo}$, for each pair of rotamers. A value of $\Delta E_{min} > 0$ indicates the endo rotamer is more stable while $\Delta E_{min} < 0$ indicates the exo rotamer is more stable. [d] $\Delta(\Delta E_{min}) = |\Delta E_{min}(\mathbf{1b})| - |\Delta E_{min}(\mathbf{1a})|$. A value of $\Delta(\Delta E_{min}) > 0$ indicates a larger energy gap for rotamers of **1b** and, hence, **1a** more likely than **1b** to be detected in two stable rotameric forms.

CH_3O, and C-8 moieties. Additional duplicate ^{13}C resonances were observed for the aromatic carbons (C-3, C-4, C-5), the amide carbonyl, and all of the guanine carbons. With the exception of the $NCOCH_2N$ methylene protons, the separation between pairs of proton absorbances was small (<0.17 ppm) and similar in magnitude for each pair of duplicate resonances (Table 2). In contrast, the separation between the two $NCOCH_2N$ methylene proton resonances was large, 0.96 ppm, with the major isomer experiencing the largest upfield shift. Duplicate resonances were not detected for any deoxyribose proton or carbon.

An NMR study was performed on **2a** observing the two C-8 proton resonances as a function of temperature in order to explain these observations. Increasing the probe temperature from 30 to 75 °C resulted in a collapse of the two resonances and, upon cooling to 30 °C, a restoration of the same two resonances in the same proportions (Figure 4). This provided evidence that **2a** was a mixture of two interconvertible rotameric forms present in a 2:1 ratio at 30 °C.

Conformational isomerism is a relatively well-known phenomenon for acetanilide and amide structures (*15*−*18*). Chupp and Olin (*15*) analyzed a series of *ortho*-substituted α-haloacetanilides by NMR techniques and

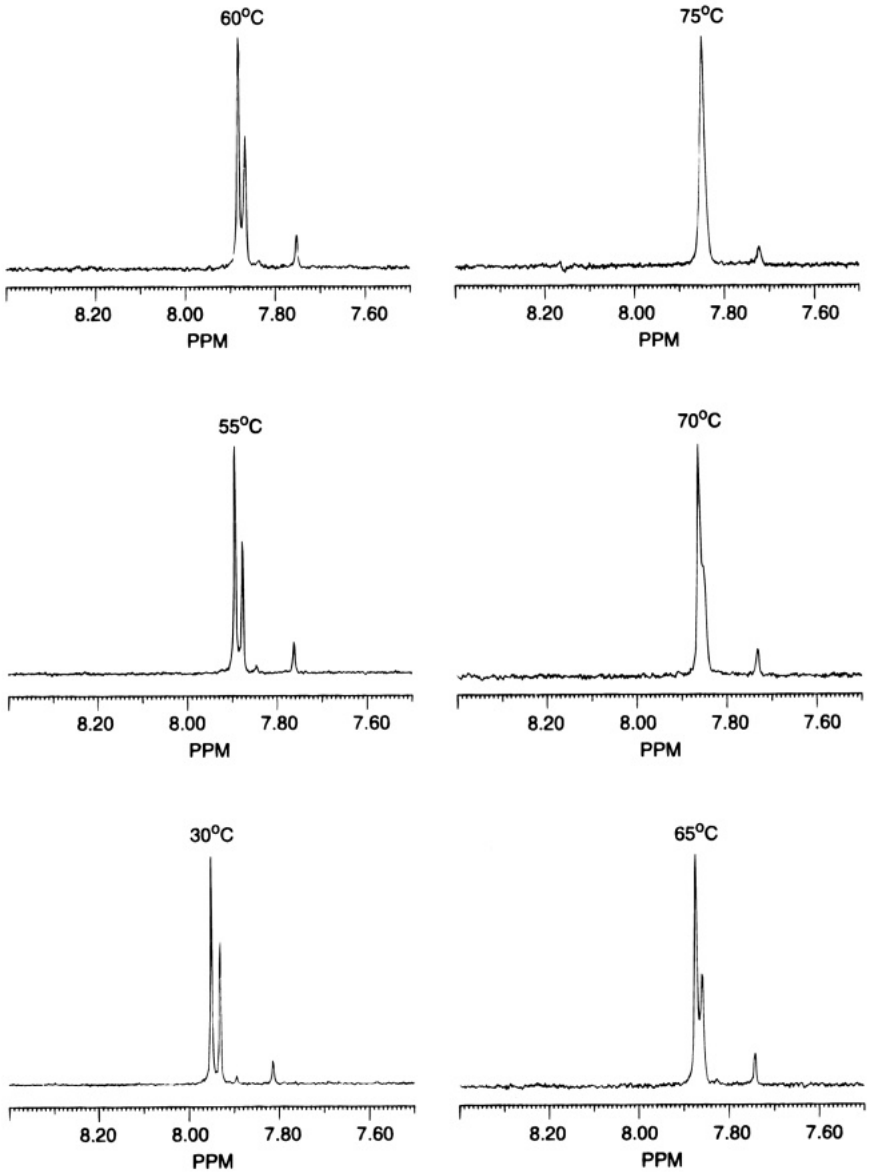

Figure 4. C-8 proton NMR absorbances of rotamers of **2a** as a function of temperature. The sample was dissolved in deuterated DMSO/water, and spectra were recorded at varying probe temperatures. Cooling the sample from 75 to 30 °C produced the original 30 °C spectrum.

reported two stable forms of those compounds containing bulky substituents on the phenyl and amide nitrogen. In more recent studies, Kovacs and Sohar (*16*) reported NMR duplicate resonances for a series of pyridinium–acetanilide salts, and Grabow *et al.* (*13*) reported a 2:1 mixture of isomers of the alachlor–GSH adduct, *S*-[[*N*-(methoxymethyl)-*N*-(2,6-diethylphenyl)carbamoyl]methyl]glutathione. The observed duplicate resonances in these studies have been attributed to a large rotational barrier about the N-carbonyl bond, a bond that is shortened due to resonance delocalization of charge from the carbonyl oxygen (*19*). Such hindered rotation gives rise to exo and endo rotamers, corresponding to the carbonyl oxygen located either *trans* or *cis* to the phenyl, respectively.

Computational studies were undertaken to investigate the nature of rotational isomerism in the 2′-deoxyguanosine adducts, **2a** and **2b**. Due to the large size and complexity of these adducts, initial computations focused on the simpler, unadducted structures, **1a** and **1b**. Analogous to the NMR spectra for **2b** and **2a, 1b** presented a single NCOCH_2Cl absorbance at 4.25 ppm

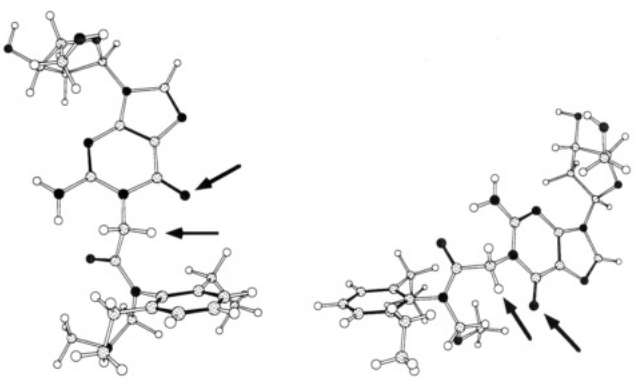

Figure 5. AM1 optimized geometries for the exo (left) and endo (right) rotamers of **2a.** Arrows point to the NCOCH_2N methylene hydrogens and the guanine carbonyl oxygen, both in close proximity to the phenyl ring in the exo configuration.

while **1a** presented duplicate resonances for the same protons at 4.33 and 3.69 ppm (in $CDCl_3$), with the latter absorbance representing the major rotamer of **1a**. These findings suggested that the minor rotamer of **1a** corresponded to the major, and only observed rotamer of **1b**.

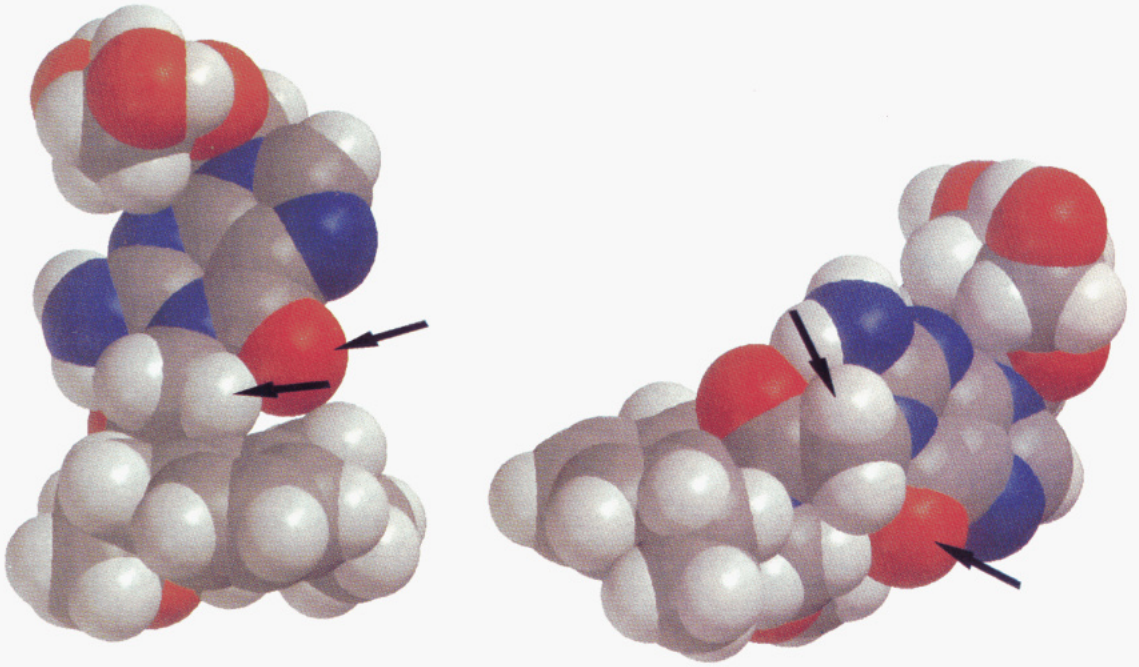

Figure 6. Space filling representations of the AM1 optimized geometries for the exo (left) and endo (right) rotamers of **2a**, corresponding to the structures presented in Figure 5: red = oxygen, blue = nitrogen, dark grey = carbon, and light grey = hydrogen. Arrows point to the NCOCH_2N methylene hydrogens and the guanine carbonyl oxygen, both in close proximity to the phenyl ring in the exo configuration.

Table 5. Computed Relative Energies of Alachlor– and CDEPA–2′-Deoxyguanosine Adducts

optimized geometry[a]	energy calculation method[b]	**2a**, ΔE_{min}[c]	**2b**, ΔE_{min}[c]	$\Delta(\Delta E_{min})$[d]
AM1	HF-631G*	−9.32	4.47	−4.85
	DMol-DND	−5.57	4.43	−1.14
PM3	HF-631G*	−7.88	3.99	−3.89
	DMol-DND	−1.65	3.03	1.38

[a] Methods used to obtain fully optimized, minimum energy geometries of rotamers with amide correction for AM1 and PM3. [b] Methods used to compute single point energies of optimized geometries. All energies in kcal/mol. [c] Difference in minimum energies, $\Delta E_{min} = E_{exo} - E_{endo}$, of two rotamers for each adduct. A value of $\Delta E_{min} > 0$ indicates the endo rotamer is more stable while $\Delta E_{min} < 0$ indicates the exo rotamer is more stable. [d] $\Delta(\Delta E_{min}) = |\Delta E_{min}(\mathbf{1b})| - |\Delta E_{min}(\mathbf{1a})|$. A value of $\Delta(\Delta E_{min}) > 0$ indicates **2a** more likely than **2b** to be detected in two stable rotameric forms.

Calculations performed at various levels of theory were used to predict optimized geometries and energies for the endo and exo rotameric forms of **1a** and **1b** (Table 4). In all cases, calculations predict the major rotamer, minimum energy form of **1a** as exo, and the major rotamer, minimum energy form of **1b** as endo. The optimized geometry of the exo rotamer of **1a** is characterized by a nearly planar amide group oriented perpendicular to the phenyl plane which places the chloromethylene hydrogens directly over the phenyl shielding region (*20*). This accounts for the large upfield shift of the NCOCH_2Cl proton NMR absorbance for the major rotamer of **1a** and is consistent with the findings of Chupp and Olin (*15*). In addition, at a sufficiently high level of theory (i.e., DMol-DND and HF6-31G*), calculations predict the difference in energy between the two rotamers, $\Delta(\Delta E_{min})$, to be larger for **1b** than for **1a**. This implies a smaller relative population of the minor rotamer of **1b** according to Boltzmann statistics. Thus, there is less probability of detecting both rotamers for **1b**, in agreement with experiment (*20*).

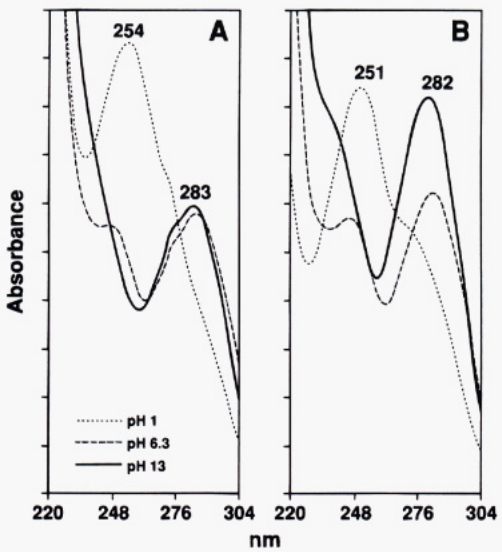

Figure 7. UV analyses of **3** at different pHs. Panel A: **3**. Panel B: 7-methylguanine.

Geometries of each rotamer of the 2′-deoxyguanosine adduct structures, **2a** and **2b**, were optimized using AM1 and PM3 semiempirical methods, and the energy of each structure was evaluated at both the ab initio DMol-DND and HF6-31G* levels (Table 5). All four method combinations (i.e., HF631G*//AM1, HF631G*//PM3, DMol//AM1, DMol//PM3) predict **2a** to prefer the exo rotamer and **2b** to prefer the endo rotamer, by a relatively large energy margin in each case. These results account for the NCOCH_2N absorbance patterns and agree with the findings for **1a** and **1b**. Note, however, that only the DMol//PM3 calculation predicts a positive value of $\Delta(\Delta E_{min})$ in Table 5, consistent with reduced likelihood of detecting duplicate resonances for **2b,** in agreement with the NMR data. The scatter in $\Delta(\Delta E_{min})$ values between the four different methods could be attributed to greater uncertainties in the computed geometries and energies

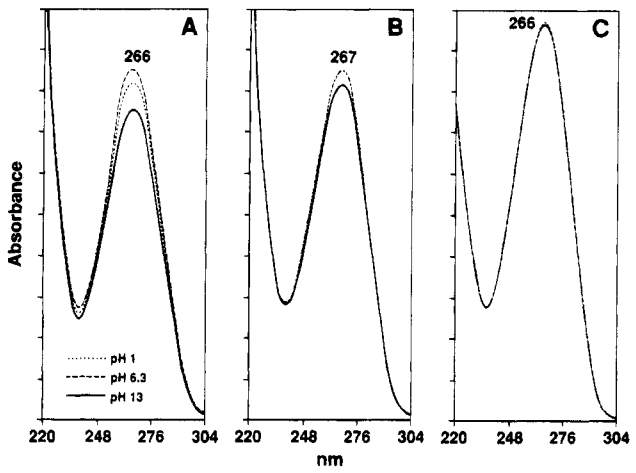

Figure 8. UV analyses of alachlor– and CDEPA–thymidine adducts at different pHs. Panel A: **4a**. Panel B: **4b**. Panel C: 3-methylthymidine. Both adducts were stable under the pH conditions used to obtain the spectra.

of the adducts, **2a** and **2b,** due to the more limited conformational search.

NMR duplicate resonance patterns observed for **2a** can be rationalized by comparison of the 3D geometries of the exo and endo rotamers in Figures 5 and 6. The $NCOCH_2N$ methylene hydrogens in the exo rotamer lie directly over the phenyl ring, with one hydrogen within the van der Waal's contact surface of a phenyl carbon [ϱ = 0.9, z = 1.0 ring radius unit (1 rru = 1.4 Å)] (*21*). Hence, these protons would experience a large upfield shift relative to the endo form. In addition, in the exo but not the endo rotamer, the guanine carbonyl oxygen is in close proximity to the phenyl ring [ϱ = 2.1, z = 2.4 rru] (*21*). This oxygen, in turn, is inductively coupled to the guanine through π electron delocalization, thus serving as a conduit between the magnetic shielding regions of the guanine and phenyl aromatic systems. This long range, delocalized interaction could account for the small, constant separations between the duplicate resonances observed for all the guanine and phenyl protons. Finally, the lack of experimentally observed duplicate resonances for the deoxyribose moiety in **2a** is explained by this group's similar orientation with respect to guanine, lack of resonance coupling to the guanine ring, and remoteness to the major shielding regions within the molecule in both rotamers.

A second product was isolated from the reaction of **1a** and 2′-deoxyguanosine. This product was identified as 7-[[*N*-(methoxymethyl)-*N*-(2,6-diethylphenyl)carbamoyl]-methyl]guanine (**3**) (Figure 1). The UV spectra of **3** at three pHs was consistent with a guanine substituted at N-7 and similar to the reference standard, 7-methylguanine (Figure 7). Proton NMR spectra identified all of the expected **1a** protons with duplicate sets of resonances for the ethyl, $NCOCH_2N$, OCH_2N, CH_3O, and C-8 protons

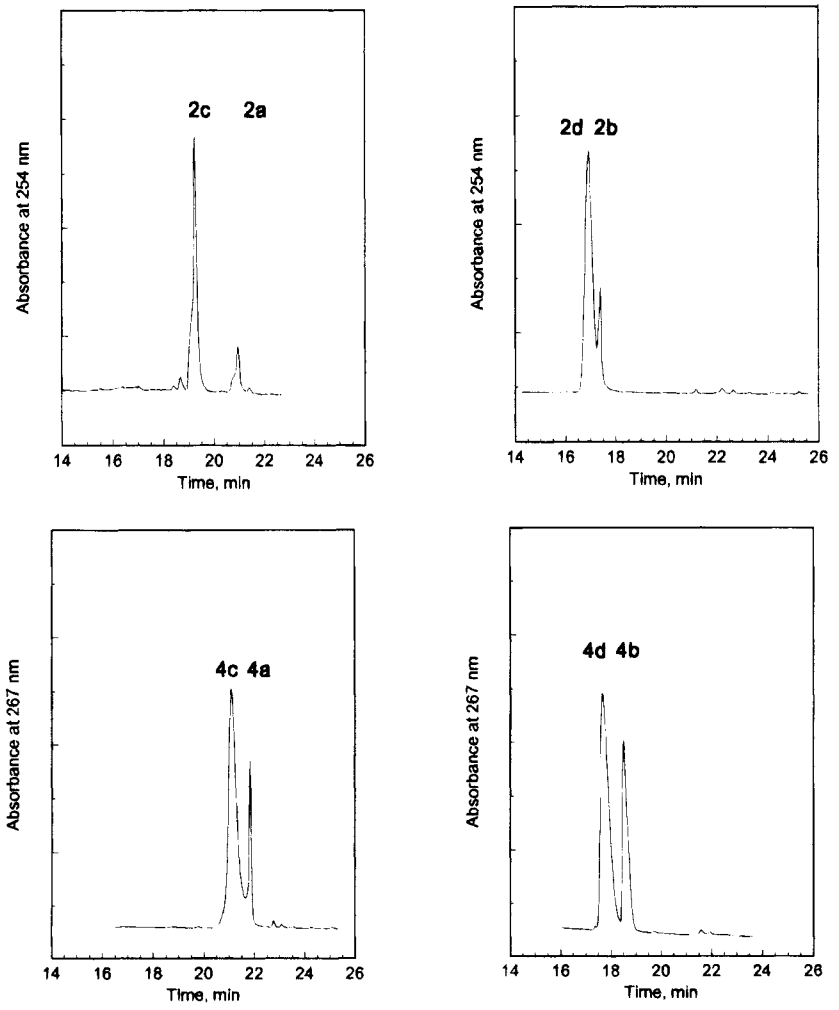

Figure 9. HPLC analyses of the incubation solution after enzymatic cleavage of alachlor and CDEPA nucleotides by nuclease P1. HPLC reverse phase chromatograms depict the results after a 2 h incubation period. Each nucleoside adduct was identified by cochromatography with standards.

as observed in **2a** in the ratio of 3:1 (Table 2). No deoxyribose protons were evident. The difference between the two $COCH_2N$ proton resonances, 4.54 and 5.46, was 0.92 ppm. All of these findings were supported by the mass spectra with the parent ion at m/z 385 $(M + H)^+$ and fragments of m/z 204 $(C_{10}H_{13}N(CO)CO + H)^+$ and 162 $(C_{10}H_{13}NCH_2 + H)^+$, and the elemental analysis.

Reaction of **1a** and **1b** with thymidine produced adducts **4a** and **4b** (Figure 1). The UV spectra of both adducts were characteristic of an N-3-substituted thymidine and identical to that of 3-methylthymidine at three pHs (Figure 8). Mass spectral fragmentations (fragments A–D) were similar to those observed with the 2′-deoxyguanosine adducts (Table 1, Figure 2). Proton and ^{13}C NMR spectra of **4a** and **4b** revealed that all the expected resonances and atom assignments were made with 2D-COSY, 2D-XHCORR, and DEPT evaluations (Tables 2 and 3). **4a** exhibited duplicate resonances for the ethyl, OCH_2N, CH_3O, and $dTCH_3$ protons in the ratio of 10:1. Duplicate resonances were not observed in the ^{13}C spectra. It is concluded that **4a** exists predominantly in one major rotameric form based on the NMR spectra.

In order to prepare 3′-monophosphate adducts for future ^{32}P-postlabeling DNA adduct studies, reactions were carried out with **1a** or **1b** and dGMP(3′) or TMP-(3′). Using a similar method of synthesis as applied to the preparation of nucleoside adducts, with the addition of reverse phase medium pressure chromatography to purify the nucleotides, four products were obtained (**2c**, **2d**, **4c**, and **4d**) (Figure 1). The nucleotide adducts exhibited the same UV spectra at three pHs as their respective nucleoside adducts (data not shown). Additional structural proof was obtained by subjecting each nucleotide adduct to the dephosphorylating action of nuclease P1, an enzyme noted for its ability to cleave nucleotide-3′ monophosphates (*8*). In each case, HPLC analyses revealed the nucleotide being cleaved to its respective nucleoside (Figure 9).

In conclusion, we have demonstrated the facile reaction of alachlor and CDEPA with nucleosides and nucleotides, characterized the nature of the adducts formed, and used computational methods to account for patterns of duplicate NMR resonances ascribed to rotational isomerism.

Acknowledgment. The authors acknowledge Dr. Ashoka Ranasinghe at the School of Public Health, University of North Carolina at Chapel Hill, for performing the precise mass determinations and Dr. Jeffrey Ross of the Carcinogenesis and Metabolism Branch, EPA, for the color graphics.

References

(1) Environmental Protection Agency (1989) Pesticide Industry Sales and Usage: 1988 Market Estimates. Office of Pesticide Programs, December, Washington, DC.
(2) Cowell, J. E., Danhaus, R. G., Kunstman, J. L. Hackett, A. G., Oppenhuizen, M. E., and Steinmetz, J. E. (1987) Operator exposure from closed system loading and application of alachlor herbicide. *Arch. Environ. Contam. Toxicol.* **16**, 327–332.
(3) Bonfanti, M., Taverna, P., Chiapetta, L., Villa, P., D'Incalci, M., Bagnati, R., and Fanelli, R. (1992) DNA damage induced by alachlor after in vitro activation by rat hepatocytes. *Toxicology* **72**, 207–219.
(4) Environmental Protection Agency (1984) Alachlor. Special Review Position Document, 1, 89 pp, Office of Pesticides and Toxic Substances, Washington, DC.
(5) Environmental Protection Agency (1987) Alachlor: Notice of Intent to Cancel Registration: Conclusions of Special Review, 118 pp, Office of Pesticides and Toxic Substances, Washington, DC.
(6) Sharp, D. B. (1981) Alachlor. In *Herbicides: Chemistry, Degradation and Mode of Action, Volume 3* (Kearney, P. C., and Kaufman, D. D., Eds.) pp 301–333, Marcel Dekker, New York.
(7) Brown, M. A., Kimmel, E. C., and Casida, J. E. (1988) DNA adduct formation by alachlor metabolites. *Life Sci.* **43**, 2087–2094.
(8) Fujimoto, M., Kuninaka, A., and Yoshino, H. (1974) Substrate specificity of nuclease P1. *Agric. Biol. Chem.* **38**, 1555–1561.
(9) Dewar, M. J. S., Zoebisch, E. G., Healy, E. F., and Stewart, J. J. P. (1985) AM1: A new general purpose quantum mechanical molecular model. *J. Am. Chem. Soc.* **107**, 3902–3909.
(10) Stewart, J. J. P. (1989) Optimization of parameters for semiempirical methods. I. Method. *J. Comput. Chem.* **10**, 209–220.
(11) Frisch, M. J., Trucks, G. W., Head-Gordon, M., Gill, P. M. W., Wong, M. W., Foresman, J. B., Johnson, B. G., Schlegel, H. B., Robb, M. A., Repogle, E. S., Gomperts, R., Andres, J. L., Raghavachari, K., Binkley, J. S., Gonzalez, C., Martin, R. L., Fox, D. J., Defrees, D. J., Baker, J., Stewart, J. J. P., and Pople, J. A. (1992) *Gaussian 92, Revision,* Gaussian, Inc., Pittsburgh, PA.
(12) DMol, Version 2.2, Quantum Chemistry Software Package, Biosym Technologies, Inc., San Diego, 1992.
(13) Grabow, J. R., Fujiwara, H., Sharp, C. R., and Logusch, E. W. (1991) Characterization of covalent protein conjugates using solid state ^{13}C NMR spectroscopy. *Biochemistry* **30**, 7057–7062.
(14) F. A. Bovey (1969) *Nuclear Magnetic Resonance Spectroscopy*, p 275, Academic Press, New York.
(15) Chupp, J. P., and Olin, J. F. (1967) Chemical and physical properties of some rotational isomers of α-haloacetanilides. A novel unreactive halogen system. *J. Org. Chem.* **32**, 2297–2303.
(16) Kovacs, Z. H., and Sohar, P. (1986) Conformational study of pyridinium–acetanilide salts by ^1H NMR spectroscopy. *Magn. Reson. Chem.* **24**, 900–902.
(17) Stewart, W. E., and Siddall, T. H., III (1970) Nuclear magnetic resonance studies of amides. *Chem. Rev.* **70**, 517–551.
(18) Oki, M. (1984) Recent advances in atropisomerism. *Top. Stereochem.* **14**, 1–81.
(19) Pauling, L. (1960) *The Nature of the Chemical Bond*, 3rd ed., *p 281 ff*, Cornell, Ithaca, NY.
(20) Richard, A., Boone, P., Padgett, W. F., and Nesnow, S. (1994) Computational studies of the conformational isomerism of alachlor and related compounds. Abstract presented at the *34th Sanibel Symposium Proceedings*, Ponte Vedra Beach, FL, Feb 12–21, 1994.
(21) Bovey, F. A. (1969) *Nuclear Magnetic Resonance Spectroscopy*, pp 64–65, Academic Press, New York.

TX940119J